Evaluation of a ^{64}Cu-labeled 1,4,7-triazacyclononane, 1-glutaric acid-4,7 acetic acid (NODAGA)-galactose-bombesin analogue as a PET imaging probe in a gastrin-releasing peptide receptor-expressing prostate cancer xenograft model

MIN HWAN KIM[1,2], JI AE PARK[1], SANG-KEUN WOO[1], KYO CHUL LEE[1], GWANG IL AN[1], BYOUNG SOO KIM[1], KWANG IL KIM[1], TAE SUP LEE[1], CHAN WHA KIM[2], KYEONG MIN KIM[1], JOO HYUN KANG[1] and YONG JIN LEE[1]

[1]Molecular Imaging Research Center, Korea Institute of Radiological and Medical Sciences (KIRAMS); [2]School of Life Sciences and Biotechnology, Korea University, Seoul, Republic of Korea

Received November 6, 2014; Accepted December 23, 2014

DOI: 10.3892/ijo.2015.2832

Abstract. Gastrin-releasing peptide receptor (GRPR) is overexpressed by a variety of human tumors and in particular, identified to be upregulated in prostate cancers. The current study aimed to develop clinically translatable BBN analogue-based radioligands for positron emission tomography (PET) of GRPR-positive tumors. We developed radiolabeled BBN analogues and modified radiolabeled galacto-BBN analogues and then investigated their tumor-targeting efficacy *in vivo*. The chelator 1,4,7-triazacyclononane, 1-glutaric acid-4,7 acetic acid (NODAGA) was used to radiolabel the peptides with ^{64}Cu. The peptides were evaluated by measuring cell-based receptor-binding affinities. Biodistribution experiments and small animal imaging using PET were performed in nude mice bearing subcutaneous PC3 human prostate cancer xenografts. The conjugates were radiolabeled with yields >99%. The stability assay showed that [^{64}Cu]NODAGA-BBN and [^{64}Cu]NODAGA-galacto-BBN remained stable in both human and mouse serum for 1 h at 37˚C. PET images of PC3 tumor-bearing nude mice were acquired at 1, 3, 24, 48 and 72 h after injection. [^{64}Cu]NODAGA-galacto-BBN showed retention in tumors for 72 h, low liver uptake, and rapid renal clearance. PET imaging results were also confirmed by biodistrubution 1 and 3 h after injection. [^{64}Cu]NODAGA-BBN and [^{64}Cu]NODAGA-galacto-BBN are promising new PET probes for GRPR-positive prostate cancer.

Correspondence to: Dr Yong Jin Lee or Dr Joo Hyun Kang, Molecular Imaging Research Center, Korea Institute of Radiological and Medical Sciences (KIRAMS), 75 Nowon-gil, Gongneung-Dong, Nowon-Gu, Seoul 139-706, Republic of Korea
E-mail: yjlee@kirams.re.kr
E-mail: kang2325@kirams.re.kr

Key words: bombesin, ^{64}Cu, positron emission tomography, prostate cancer, radiopharmaceuticals

Introduction

Prostate cancer is the second most frequently diagnosed cancer in men (914,000 new cases, 13.8% of the total), the fifth most common cancer across both genders, and the sixth leading cause of death from cancer in men in 2008 (1). Hormone ablation therapy is a first-line treatment for prostate cancer; however, the duration of remission is limited and androgen-independent regrowth is observed in most patients (2). Additionally, most chemotherapeutic agents provide only a marginal benefit of survival or quality of life. Therefore, the development of early diagnostic imaging agents and effective therapeutics for prostate cancer is important for prolongation of survival time and enhancement of patient quality of life.

Somatostatin and bombesin/gastrin-releasing peptide (BBN/GRP) receptors are highly expressed in prostate cancers and can be selectively targeted by cytotoxic peptide conjugates. Peptide analogues are an exciting potential treatment for androgen-independent prostate cancer (3). BBN is a 14-amino-acid neuropeptide, first isolated from frog skin (4,5), and it has high affinity for the gastrin-releasing peptide receptor (GRPR). BBN and its mammalian counterpart, GRP, have similar biological properties and share nearly identical C-terminal amino acid sequences. In prostate cancer, GRPR expression is closely associated with neoplastic transformation (6), cell migration (7,8), proliferation (6,9), and invasion capacity (10,11).

GRPR is an important target for radiolabeled BBN analogues that function as diagnostics or radionuclide therapies for GRPR-positive tumors (12). Various BBN analogues have been labeled with radiometals and suitable chelators and used for positron emission tomography (PET) imaging in GRPR-positive tumors (13-15). ^{99m}Tc-labeled BBN analogues have been synthesized with diaminedithiol (DADT) and the dithiadiphosphine framework (P_2S_2-COOH) as chelators. These analogues were evaluated in normal mice (16,17) and PC3 tumor-bearing mice, which represented a model of prostate cancer (18,19). Bifunctional chelators and linkers are

necessary for specific uptake into the tumors and to reduce uptake of radiometals into normal tissue. Rogers *et al* labeled 1,4,7,10-tetraazacyclododecane-N,N',N'',N'''-tetraacetic acid (DOTA)-Aoc is 8-aminooctanoic acid (Aoc)-BBN(7-14) with ^{64}Cu and then applied this radiotracer to a PC3 xenograft model (20). The tumor was well-visualized; however, sustained blood concentrations and persistent liver and kidney retention limited the potential clinical application of this tracer.

Peptides as targeting molecules have unique characteristics *in vivo* including fast washout and excretion via the kidney because of their hydrophilic nature. To modulate the pharmacokinetic characteristics of radiolabeled peptide *in vivo*, researchers have tried to optimize to lower uptake in non-target organ and higher in target organ by modification of chelator and linker. Parry *et al* reported that shorter aliphatic linkers (from C4 to C12) between the DOTA and BBN resulted in lower liver uptake with simultaneous higher uptake into GRPR-positive breast tumors (21). Another group applied 1,4,7-triazacyclononane-1,4-diacetic acid (NO2A) and various aliphatic linkers as a 1,4,7-triazacyclononane-1,4,7-triacetic acid (NOTA) derivative chelator and a pharmacokinetic modifier to BBN for ^{64}Cu labeling to improve tumor uptake and pharmacokinetic properties, respectively. They reported that shorter and more hydrophilic linker produced superior small animal PET images, with minimal accumulation in collateral tissue but the longer and more lipophilic linker resulted in high accumulation of radioactivity in liver and abdominal region (22). Parry *et al* introduced short peptides as a linker between DOTA and BBN to reduce retention of the tracer in the liver by activating the hepatobiliary pathway (23). Glycosylating the peptides is an alternative strategy to improve pharmacokinetic properties (24,25). Arg-Gly-Asp (RGD) peptide conjugates ([$^{123\ or\ 125}$I]Gluco-RGD (25) and [^{18}F] Galacto-RGD) (24,26,27), which can be used to target new vascularization in tumors, showed very similar kinetics in the kidney. In addition, RGD peptide conjugates displayed clearly reduced activity in the liver as well as increased uptake and retention in the tumor compared with the unmodified parent peptides. ^{64}Cu is widely used because it is easy to produce with a medical cyclotron (28). ^{64}Cu can be used in PET to evaluate the kinetics of protein or peptide interactions with target cells, and has a suitable positron energy (17.8%, E_{β^+max}=656 keV), and a β^- emitter (39.6%, E_{β^-max}=573 keV) with a relatively long half-life (12.7 h) (29).

In this study, we evaluated ^{64}Cu-labeled 1,4,7-triazacyclononane, 1-glutaric acid-4,7 acetic acid (NODAGA)-BBN and ^{64}Cu-labeled NODAGA-galacto-BBN in an *in vitro* receptor-binding assay and for *in vivo* tumor targeting by visualizing PC3 prostate xenograft tumors with small animal PET.

Materials and methods

Materials. All reagents were purchased from commercial sources and used as received without further purification. NODAGA-BBN(7-14)NH_2 and NODAGA-galacto-BBN(7-14) NH_2 were obtained from AnyGen Co., Ltd. (Jeollanam-do, Korea). [^{125}I]Tyr^4-BBN(1-14) was obtained from PerkinElmer, Inc. (Branford, CT, USA). Ham's F-12K medium was purchased from WelGENE, Inc. (Daegu, Korea). Bovine serum albumin (BSA), $CaCl_2$, glacial acetic acid, NaCl, NaOH, $MnCl_2$, penicillin, phosphate-buffered saline (PBS), sodium acetate, streptomycin, and tris(hydroxymethyl)aminomethane (Tris) were purchased from the Sigma-Aldrich Corp. (St. Louis, MO, USA). Matrigel (BD Matrigel Basement Membrane Matrix) was purchased from BD Biosciences (San Jose, CA, USA). Instant Thin Layer Chromatography-Silica Gel (ITLC-SG) was purchased from Agilent Technologies, Inc. (Santa Clara, CA, USA). Antibiotics and antimycotics, including amphotericin B, streptomycin, and penicillin, were purchased from Invitrogen Life Technologies (Carlsbad, CA, USA). The PC3 human prostate cancer cell line was obtained from the American Type Culture Collection (Manassas, VA, USA).

High-performance liquid chromatography and mass spectrometry. The purity of NODAGA-BBN(7-14)NH_2 and NODAGA-galacto-BBN(7-14)NH_2 was analyzed using high-performance liquid chromatography (HPLC) (Shimadzu HPLC 10AVP system) with a C18 analytical column (5 μm, 3.0x150 mm). The elution conditions were as follows: a mixture of an aqueous solution of solvent A [0.1% trifluoroacetic acid (TFA) in acetonitrile] and B (0.1% TFA in water) with a 30-min linear gradient from 5 to 65% at a flow rate of 1 ml/min. Matrix-assisted laser desorption/ionization (MALDI) and MALDI time-of-flight (MALDI-TOF) experiments were performed on a Kratos Shimadzu Axima-CFR.

Synthesis. Solid-phase peptide synthesis (SPPS) was performed on a PIT-Symphony Peptide Synthesizer using the 9-fluorenylmethoxycarbonyl (Fmoc) methodology to produce the BBN(7-14)NH_2 peptide (22). Conjugation of NODAGA to the BBN(7-14)NH_2 peptide resulted in NODAGA-BBN(7-14)NH_2 via an active ester. A solution of NODAGA (286 μmol) in dimethylformamide (DMF) (1 ml) and N,N-diisopropylethylamine (DIEA) (2 M, 800 μl) was added on the resin with stirring at room temperature (RT). The stirring was continued for 12 h, after which the resin was washed three times with DMF. Fmoc deprotection was performed in 20% piperidine; subsequently, the resin was washed three times with DMF. The NODAGA-BBN(7-14)NH_2 was isolated by HPLC.

The preparation of NODAGA-galacto-BBN(7-14)NH_2 was essentially similar to the preparation of NODAGA-BBN(7-14) NH_2 described above. Galacturonic acid was conjugated via an active ester onto the amine of glutamine (Q) on the BBN(7-14)NH_2. To a mixture of galacturonic acid (10 μmol) in DMF (140 μl), hydroxybenzotriazole (HOBt) (2 M, 40 μl) and 1,3-diisopropylcarbodiimide (DIC) (2 M, 40 μl) were added on the resin with stirring at RT. The stirring was continued for 12 h, after which the resin was washed three times with DMF. Fmoc deprotection was performed in 20% piperidine, and the resin was washed three times with DMF. A solution of NODAGA (286 μmol) in DMF (1 ml) and DIEA (2 M, 800 μl) was added to the resin with stirring at RT for 12 h. NODAGA-galacto-BBN(7-14)NH_2 was isolated by HPLC. HPLC analysis and mass spectroscopy were used to confirm the identity of the product.

Preparation of [^{64}Cu]NODAGA-BBN and [^{64}Cu]NODAGA-galacto-BBN. ^{64}Cu was produced at the Korea Institute of Radiological and Medical Sciences (KIRAMS) (Seoul,

Korea) with 50 MeV of cyclotron irradiation using methods reported previously (30). The solvent was evaporated for 30 min under a stream of argon at 110˚C. To prepare the [^{64}Cu]NODAGA-BBN and [^{64}Cu]NODAGA-galacto-BBN, a ^{64}Cu solution (74-185 MBq) was added to a solution of NODAGA-BBN and NODAGA-galacto-BBN (24 μg/1 ml 0.2 M sodium acetate buffer, pH 4.0) in a glass vial. The resulting mixture was shaken at 70˚C for 20 min. Subsequently, ^{64}Cu incorporation was determined by radio-thin layer chromatography (radio-TLC).

Cell culture and cell binding assay. The human prostate cancer PC3 cell line cultured in Ham's F-12K medium containing 20% (v/v) FBS and 1% (v/v) penicillin/streptomycin solution. Cultures were maintained in a 37˚C incubator with 5% CO_2 in air, and the medium was changed every 3 days.

Cell binding assays for [^{64}Cu]NODAGA-BBN or [^{64}Cu] NODAGA-galacto-BBN on PC3 cells were performed as described previously (13). PC3 cells ($2x10^6$/100 μl) were resuspended in binding buffer (Ham's F-12K medium containing 20 mM Tris, pH 7.4, 150 mM NaCl, 2 mM $CaCl_2$, 1 mM $MnCl_2$, and 0.1% BSA). For the assay, equal volumes of non-radioactive ligands (NODAGA-BBN or NODAGA-galacto-BBN) and radioactive ligand (3.7 MBq [^{125}I]Tyr^4-BBN; PerkinElmer, Inc., Waltham, MA, USA) were added. The GRPR ligands were added at concentrations 10^{-4}-10^{-13} M. The tubes were incubated for 60 min at RT. Then, the reaction medium was removed and the cells were washed three times with cold PBS. The cells were harvested and the bound radioactivity was counted with a gamma counter (1480 Wizard 3'' Automatic Gamma Counter; PerkinElmer, Inc.). Data were analyzed with GraphPad Prism 5 (GraphPad Software, Inc., San Diego, CA, USA) to determine the half maximal inhibitory concentration (IC_{50}) value. Experiments were performed in triplicate.

Partition coefficient determination. The octanol/water partition coefficient of [^{64}Cu]NODAGA-BBN and [^{64}Cu] NODAGA-galacto-BBN was determined using the following protocol. Approximately 3.7 MBq of [^{64}Cu]NODAGA-BBN or [^{64}Cu]NODAGA-galacto-BBN in 3 ml of PBS (pH 7.4) was added to 4 ml of octanol. The mixture was then vigorously stirred for 5 min and centrifuged (3,000 rpm, 5 min). The activity of both the PBS and octanol phases was measured in the gamma counter, and logP values were calculated (n=3).

Internalization studies and in vitro stability of [^{64}Cu] NODAGA-BBN and [^{64}Cu]NODAGA-galacto-BBN in human serum. Internalization studies for [^{64}Cu]NODAGA-BBN or [^{64}Cu]NODAGA-galacto-BBN on PC3 cells were performed as described previously (18,19). One million PC3 cells per tube were prepared for internalization studies. The cells were washed with PBS and then incubated with [^{64}Cu]NODAGA-BBN or [^{64}Cu]NODAGA-galacto-BBN (0.0001 MBq/tube) for 2 h at 4˚C. To remove unbound radioactivity, the cells (n=3) were washed twice with ice-cold PBS and incubated with prewarmed culture medium at 37˚C for 0, 5, 15, 30, 45, 60, 90, and 120 min to allow internalization.

To remove cell surface-bound radiotracer, the cells were washed twice with acid (50 mM glycine-HCl/100 mM NaCl, pH 2.8). The acid solution was collected, and radioactivity was measured with the gamma counter. The results were measured as surface-bound activity. The cells were treated with 1 M NaOH, and the resulting lysate was then measured with the gamma counter. The results are expressed as the percentage of internalized activity relative to the total activity (surface-bound activity + internalized activity). The results are expressed as the mean ± standard deviation (SD).

The stability of compounds [^{64}Cu]NODAGA-BBN and [^{64}Cu]NODAGA-galacto-BBN was assessed with a radio-TLC scanner and instant TLC (ITLC) paper. Either [^{64}Cu]NODAGA-BBN or [^{64}Cu]NODAGA-galacto-BBN (185 MBq/50 μl) was incubated at 37˚C in 1 ml of human serum and mouse serum for different time intervals (1, 4 and 24 h). Free ^{64}Cu was used as a reference. The mobile phase consisted of 20 mM sodium acetate and 50 mM EDTA (pH 5.0). ITLC was performed using a radio-TLC scanner (Aloka, Tokyo, Japan).

Pharmacokinetic study of [^{64}Cu]NODAGA-BBN and [^{64}Cu] NODAGA-galacto-BBN. The care, maintenance, and treatment of animals in these studies followed protocols approved by the Institutional Animal Care and Use Committee (IACUC) of the KIRAMS (IACUC no. KIRAMS 2013-80). Female nude mice (BALB/cSlc-nu/nu, 6-weeks old) were purchased from Japan SLC, Inc. (Shizuoka, Japan). Animals were maintained in a temperature-controlled chamber at 22±3˚C with a 12-h light/dark cycle. Relative humidity was maintained at 55±20%. Sterilized rodent diet and purified tap water were supplied *ad libitum*. Animals were acclimatized to the condition described above for a week prior to use for the study.

Nude mice received [^{64}Cu]NODAGA-BBN or [^{64}Cu] NODAGA-galacto-BBN via their tail veins at 7.4 MBq/head dose (n=6 each). Blood samples were collected from retro-orbital plexus via the sodium-heparinized capillary tube (75 mm; Paul Marienfeld GmbH & Co. KG, Lauda-Königshofen, Germany) at 0, 0.0833, 0.167, 0.25, 0.5, 1, 2, 4, 6, 8 and 24 h after administration. Dosing solution (20 μl) and blood samples (50 μl) were transferred to polyethylene tubes. Each radioactivity of them was counted by a scintillation counter. The radioactivity concentration of blood sample was expressed as the percentage of injected dose per a milliliter of blood (% ID/ml).

Pharmacokinetic parameters were estimated from the blood radioactivity concentration vs. time data by non-compartmental method using the non-linear least-squares regression program, WinNonlin ver. 2.0 (Pharsight Corp., Cary, NC, USA).

Biodistribution studies. Male athymic nude (Nu/Nu) BALB/c mice (Nara Biotech Co., Ltd., Seoul, Korea) were injected subcutaneously with $1x10^7$ PC3 human prostate cancer cells suspended in 100 μl of a Matrigel and PBS mixture (Matrigel:PBS = 1:1) at 6 weeks of age in the flank of the left thigh. The mice were subjected to biodistribution studies and PET imaging when the tumor reached 0.7-0.9 cm in diameter (18-21 days after implantation).

The PC3 tumor-bearing nude mice (n=3 for each group) were injected with ~1.48 MBq of [^{64}Cu]NODAGA-BBN or [^{64}Cu]NODAGA-galacto-BBN via the tail vein and sacrificed at 1 or 3 h after injection. The tumor and normal tissues of interest were removed and weighed, and their radioactivity

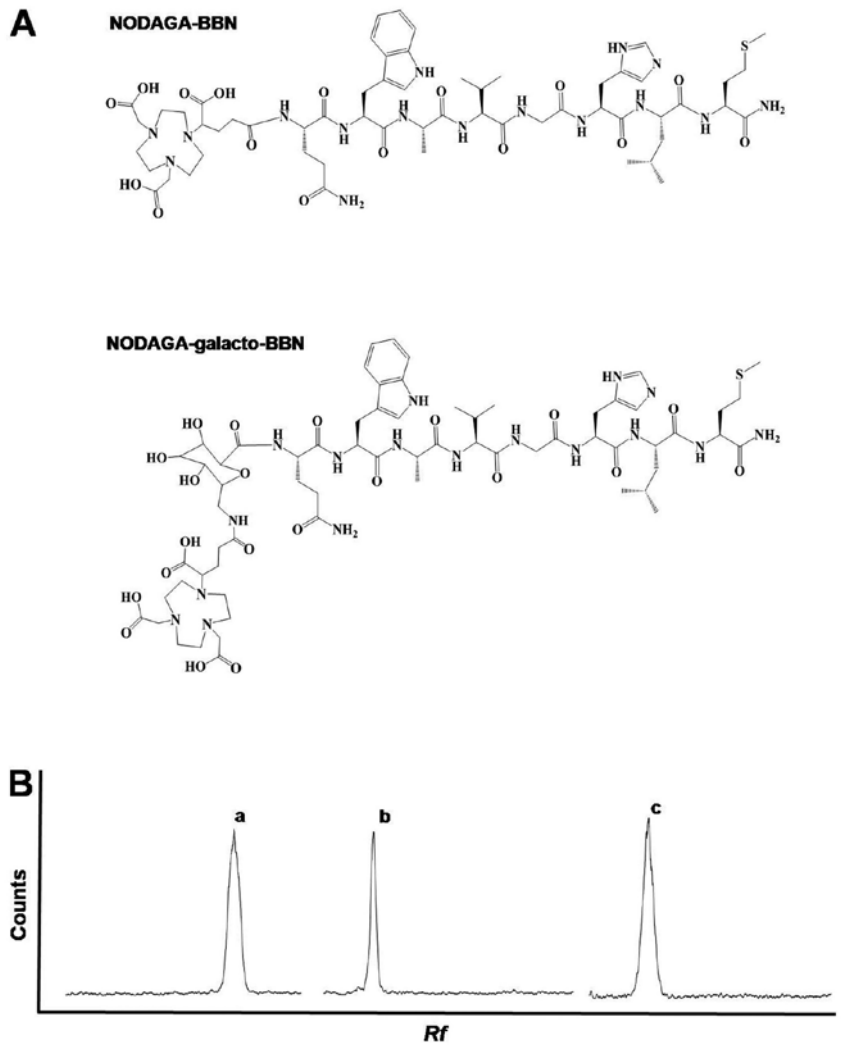

Figure 1. *In vitro* characterization of the BBN analogues. (A) Chemical structure of 1,4,7-triazacyclononane, 1-glutaric acid-4,7 acetic acid (NODAGA)-BBN and NODAGA-galacto-BBN. (B) Radio-thin-layer chromatography (radio-TLC) of (a) ^{64}Cu, (b) [^{64}Cu]NODAGA-BBN, and (c) [^{64}Cu]NODAGA-galacto-BBN.

levels were measured using a gamma counter. The uptake of radioactivity in the tumor and normal tissues was expressed as percent of injected dose per gram (% ID/g).

Small animal PET studies. Whole-body PET images were obtained using a dedicated small animal PET/CT scanner (Inveon™; Siemens Preclinical Solutions, Malvern, PA, USA). Animals were anesthetized with 1.5% isoflurane (Foran; Choongwae Pharma Co., Seoul, Korea) and injected with 11.1-18.5 MBq (100 μl) of [^{64}Cu]NODAGA-BBN or [^{64}Cu] NODAGA-galacto-BBN via the caudal vein, and 30-min static scans were acquired at 1, 3, 24, 48 and 72 h after injection. *In vivo* GRPR-blocking experiment performed to confirm specific tumor-targeting efficiency. To block GRPR, 15 mg/kg of NODAGA-BBN or NODAGA-galacto-BBN intravenously injected 30 min ahead of [^{64}Cu]NODAGA-BBN or [^{64}Cu] NODAGA-galacto-BBN injection, then PET images were acquired at 1 h after injection. PET images were reconstructed using an ordered subset expectation maximization (OSEM) 2D algorithm with four iterations. Regions of interest (ROIs) were drawn on the reconstructed images using Inveon Research Workplace (IRW), provided by Siemens Preclinical Solutions.

Statistical analysis. Data were analyzed with GraphPad Prism statistical software (GraphPad Software, Inc.). Student's two-tailed t-test was used to determine statistical significance at the 95% confidence level, with $P<0.05$ considered significantly different.

Results

Chemistry and radiochemistry. The NODAGA-BBN(7-14) NH_2 conjugate was obtained with a 97.2% yield and a 19.2-min retention time (Rt) on analytical HPLC. The MALDI-TOF mass of NODAGA-BBN(7-14)NH_2 was m/z=1298.3 (calculated for $C_{58}H_{88}N_{16}O_{16}S_1$, 1297.5) (Table I).

The NODAGA-galacto-BBN(7-14)NH_2 conjugate was obtained in 95.2% yield with a 19.8-min Rt on analytical HPLC. The MALDI-TOF mass of NODAGA-galacto-BBN(7-14) NH_2 was m/z=1487.2 (calculated for $C_{65}H_{99}N_{17}O_{21}S_1$, 1486.6) (Table I). NODAGA-BBN and NODAGA-galacto-BBN were labeled with ^{64}Cu at 70˚C for 20 min. The final products of the NODAGA-BBN and NODAGA-galacto-BBN complexes are shown in Fig. 1A. The radiolabeling yields of NODAGA-BBN and NODAGA-galacto-BBN were >99% (Table I and Fig. 1B).

Table I. The MALDI-TOF mass of NODAGA.

	NODAGA-BBN	NODAGA-galacto-BBN
Chemical formula	$C_{58}H_{88}N_{16}O_{16}S_1$	$C_{65}H_{99}N_{17}O_{21}S_1$
Calculated MW	1297.5	1486.6
MALDI-TOF mass	1298.3	1487.2
LogP	-3.09±0.03	-3.29±0.08
Radiolabeling efficiency (%)	100±0.00	100±0.00

MALDI-TOF, matrix-assisted laser desorption/ionization time-of-flight; NODAGA, 1,4,7-triazacyclononane, 1-glutaric acid-4,7 acetic acid; MW, molecular weight.

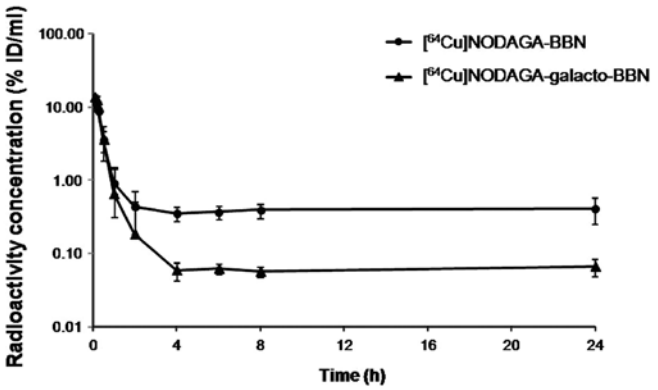

Figure 2. Average blood radioactivity concentration versus time curves obtained in nude mice after intravenous (i.v.) injection of [^{64}Cu]1,4,7-triazacyclononane, 1-glutaric acid-4,7 acetic acid (NODAGA)-BBN or [^{64}Cu]NODAGA-galacto-BBN (injected dose: 200 μCi/head, n=6). Values are represented as mean % ID/ml ± standard deviation (SD). % ID/ml, the percent-injected dose per a milliliter of blood.

Pharmacokinetic study of [^{64}Cu]NODAGA-BBN and [^{64}Cu]NODAGA-galacto-BBN. The blood radioactivity concentration-time profiles following single intra-venous (i.v.) bolus injection of [^{64}Cu]NODAGA-BBN or [^{64}Cu]NODAGA-galacto-BBN in nude mice are shown in Fig. 2. In both, the blood radioactivity concentrations decreased biexponentially and reached the steady state at 4 h after administration. At the steady state, the blood radioactivity level of [^{64}Cu]NODAGA-BBN was ~6 times higher than that of [^{64}Cu]NODAGA-galacto-BBN. Table II summarizes the blood pharmacokinetic parameters obtained by non-compartmental analysis. The blood concentration extrapolated to time zero (C_0) was 15.8±1.74 and 16.2±1.48% ID/ml, the terminal elimination half-life ($t_{1/2,z}$) was 70.7±43.71 and 29.2±20.61 h, and the area under blood concentration-time curve ($AUC_{0\text{-}24h}$) was 14.6±3.00 and 7.44±2.02% ID·h/ml, respectively, after i.v. injection of [^{64}Cu]NODAGA-BBN or [^{64}Cu]NODAGA-galacto-BBN. The volume of distribution at terminal phase (V_z) was 195±75.04 and 395±171.95 ml, the systemic clearance (Cl) was 2.22±0.96 and 10.3±2.89 ml/h, and the mean retention time (MRT) was 7.87±0.87 and 2.70±0.24 h, respectively, after i.v. injection of [^{64}Cu]NODAGA-BBN or [^{64}Cu]NODAGA-galacto-BBN.

Table II. Non-compartmental pharmacokinetic parameters of radioactivity in blood obtained after i.v. injection of [^{64}Cu]NODAGA-BBN or [^{64}Cu]NODAGA-galacto-BBN (injected dose: 7.4 MBq/head) in nude mice (n=6 each).

Parameter	[^{64}Cu]NODAGA-BBN	[^{64}Cu]NODAGA-galacto-BBN
C_0 (% ID/ml)	15.8±1.74	16.2±1.48
$t_{1/2,z}$ (h)	70.7±43.71	29.2±20.61
$AUC_{0\text{-}24\,h}$ (% ID·h/ml)	14.6±3.00	7.44±2.02
V_z (ml)	195±75.04	395±171.95
Cl (ml/h)	2.22±0.96	10.3±2.89
MRT_{last} (h)	7.87±0.87	2.70±0.24

i.v., intravenous; NODAGA, 1,4,7-triazacyclononane, 1-glutaric acid-4,7 acetic acid; C_0, blood concentration extrapolated to time zero; $t_{1/2,z}$, terminal elimination half-life; $AUC_{0\text{-}24\,h}$, area under blood concentration-time curve; V_z, volume of distribution at terminal phase; Cl, systemic clearance; MRT, mean retention time.

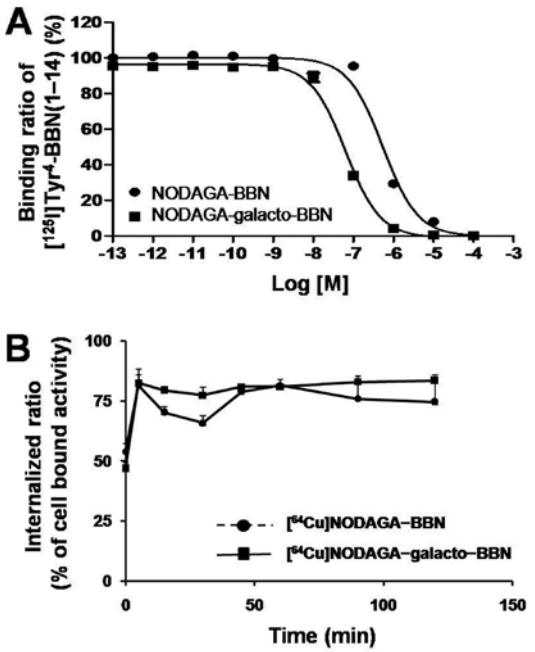

Figure 3. (A) *In vitro* cell binding assay and (B) *in vitro* internalization assay of BBN analogues. (A) Inhibition of [^{125}I]Tyr^4-BBN(1-14) binding to PC3 cells with various concentrations of 1,4,7-triazacyclononane, 1-glutaric acid-4,7 acetic acid (NODAGA)-BBN (n=3) (closed circle) and NODAGA-galacto-BBN (closed square). The data are presented as the mean ± standard deviation (SD) (n=3). (B) Internalization data for [^{64}Cu]NODAGA-BBN (closed circle) and [^{64}Cu]NODAGA-galacto-BBN (closed square) in PC3 cells. The data are presented as the mean ± SD (n=3).

In vitro characterization. The stability of [^{64}Cu]NODAGA-BBN and [^{64}Cu]NODAGA-galacto-BBN, in terms of the percentage of the intact conjugate, was measured in human or mouse serum. No de-radiometallation or major degradation of the BBN tracer was detected after incubation with human and mouse sera at 37˚C for 1 h as monitored by radio-TLC.

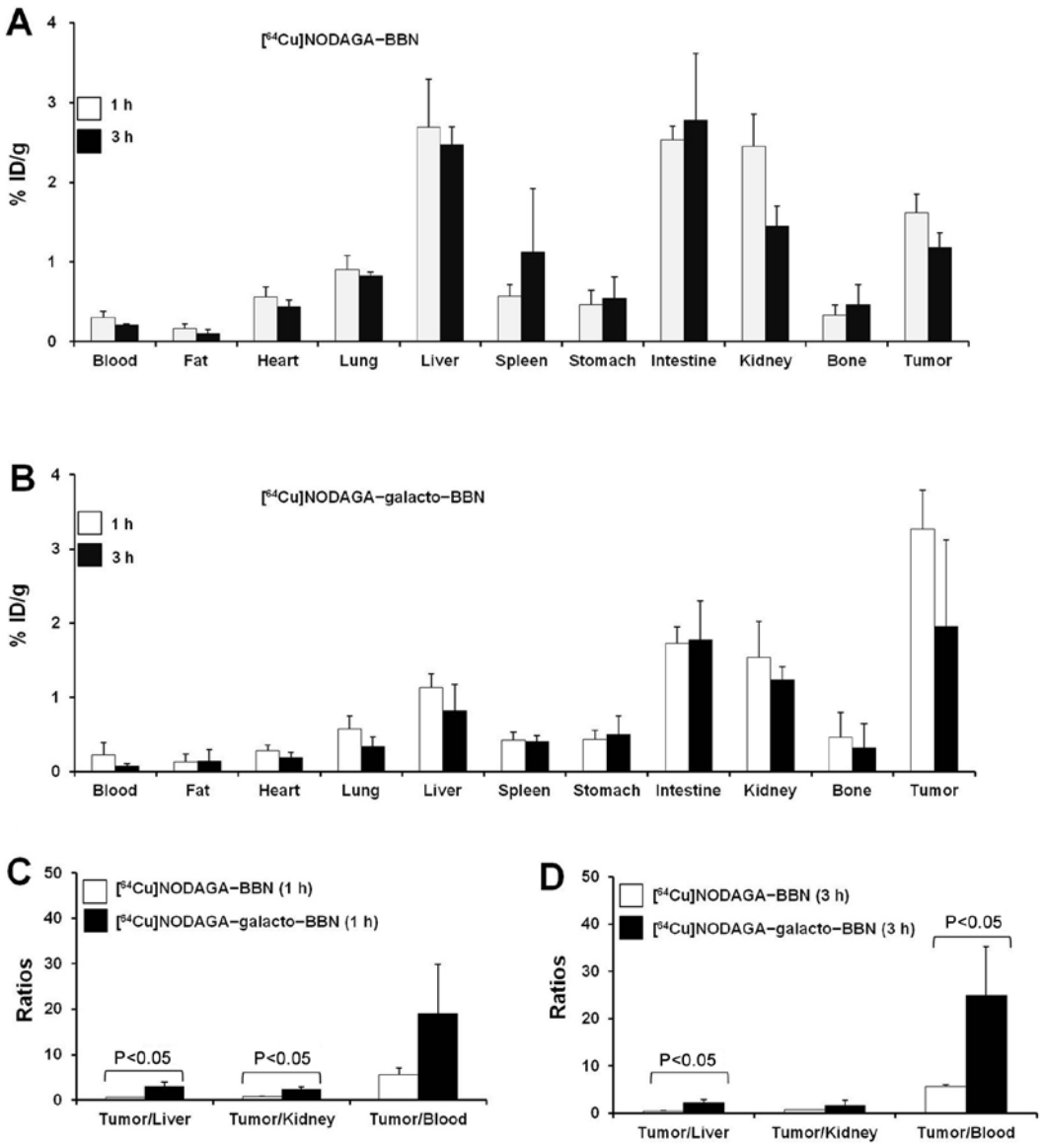

Figure 4. (A and B) Biodistribution and (C and D) calculated tumor-to-normal tissue uptake ratios for [^{64}Cu]1,4,7-triazacyclononane, 1-glutaric acid-4,7 acetic acid (NODAGA)-BBN and [^{64}Cu]NODAGA-galacto-BBN in PC3 tumor-bearing mice. (A and B) Biodistribution data of (A) [^{64}Cu]NODAGA-BBN (n=3) and (B) [^{64}Cu]NODAGA-galacto-BBN (n=3), 1 h (open bar) and 3 h (closed bar) after BBN probe injection. The data are presented as percent of injected dose per gram (% ID/g) [mean ± standard deviation (SD)]. (C and D) Tumor-to-normal tissue (liver, kidney, and blood) uptake ratios for [^{64}Cu]NODAGA-BBN (open bar, n=3) and [^{64}Cu]NODAGA-galacto-BBN (closed bar, n=3) at (C) 1 h and (D) 3 h after tracer injection. Data are presented as the mean ± SD, P<0.05 ([^{64}Cu]NODAGA-BBN vs. [^{64}Cu]NODAGA-galacto-BBN).

Cell binding assays with NODAGA-BBN and NODAGA-galacto-BBN showed that both compounds inhibited the binding of [^{125}I]Tyr^4-BBN to PC3 cells in a concentration-dependent manner. As shown in Fig. 3A, the calculated IC_{50} value of NODAGA-BBN was 547±38.9 nM, whereas a somewhat higher affinity (64.1±6.34 nM) was observed for NODAGA-galacto-BBN.

Both [^{64}Cu]NODAGA-BBN and [^{64}Cu]NODAGA-galacto-BBN showed similar logP values of -3.09±0.03 and -3.29±0.08, respectively, indicating that the complexes were highly hydrophilic and that adding the galactose moiety made the peptide even more hydrophilic.

The internalization studies presented in Fig. 3B showed that [^{64}Cu]NODAGA-BBN and [^{64}Cu]NODAGA-galacto-BBN are rapidly taken up (within 5 min) into PC3 cells. The intracellular uptake of [^{64}Cu]NODAGA-BBN and [^{64}Cu]NODAGA-galacto-BBN reached a plateau at 15 min; 75-80% of cell-bound activity was attributed to the internalization of the peptides in the cells.

Biodistribution studies. The *in vivo* uptake of [^{64}Cu]NODAGA-BBN and [^{64}Cu]NODAGA-galacto-BBN into several organs, including a GRPR-expressing PC3 prostate tumor, was measured at 1 and 3 h after i.v. injection (Fig. 4). Rapid blood clearance was observed for both [^{64}Cu]NODAGA-BBN and [^{64}Cu]NODAGA-galacto-BBN, with <0.5% ID/g remaining. Liver uptake of the [^{64}Cu]NODAGA-galacto-BBN-injected group was relatively low (1 h, 1.13±0.19% ID/g; 3 h, 0.82±0.35% ID/g) (1 h, P<0.05; 3 h, P<0.01), compared with the [^{64}Cu]NODAGA-BBN-injected group (1 h, 2.69±0.60% ID/g; 3 h, 2.47±0.23% ID/g). However, the tumor uptake of [^{64}Cu]NODAGA-galacto-BBN was significantly greater (P<0.01)

than that of [^{64}Cu]NODAGA-BBN; the tumor uptake at 1 and 3 h for [^{64}Cu]NODAGA-galacto-BBN was 3.26±0.53 and 1.96±1.16% ID/g, respectively, whereas the tumor uptake at 1 and 3 h for [^{64}Cu]-NODAGA-BBN was 1.62±0.23 and 1.18±0.18% ID/g, respectively. There was a significant difference in uptake pattern between [^{64}Cu]NODAGA-BBN and [^{64}Cu]NODAGA-galacto-BBN in other organs including the blood, heart, lungs, and intestines (Fig. 4A and B). At 1 and 3 h, the ratio of tumor to non-target (i.e., liver, kidney, and blood) for [^{64}Cu]NODAGA-galacto-BBN was higher than that of [^{64}Cu]NODAGA-BBN (Fig. 4C and D). Therefore, [^{64}Cu]NODAGA-galacto-BBN has a higher targeting efficiency than [^{64}Cu]NODAGA-BBN.

Small animal PET imaging studies. To evaluate the *in vivo* kinetics of [^{64}Cu]NODAGA-BBN and [^{64}Cu]NODAGA-galacto-BBN, small animal PET imaging studies were performed in PC3 prostate cancer-bearing mice. Fig. 5 shows a single slice of the transverse and coronal small animal PET images of a representative mouse at 1, 3, 24, 48 and 72 h after injection of [^{64}Cu]NODAGA-BBN or [^{64}Cu]NODAGA-galacto-BBN. [^{64}Cu]NODAGA-BBN and [^{64}Cu]NODAGA-galacto-BBN exhibited high tumor uptake at 1 h; the location of tumor was clearly visible for 72 h (Fig. 5A and C). Although differences of tumor uptake between two probes were not statistically significant by quantitative ROI analysis ($P>0.05$, from 1 to 72 h), liver uptake of [^{64}Cu]NODAGA-galacto-BBN was significantly lower than that of [^{64}Cu]NODAGA-BBN throughout the scanning periods ($P<0.05$, from 1 to 72 h). Tumor and liver uptake of [^{64}Cu]NODAGA-BBN and [^{64}Cu]NODAGA-galacto-BBN longitudinally decreased >72 h (Fig. 5B and D). Tumor uptake of [^{64}Cu]NODAGA-BBN or [^{64}Cu]NODAGA-galacto-BBN was barely detectable upon administration of 15 mg/kg NODAGA-BBN or NODAGA-galacto-BBN as a blocking agent 30 min before tracer injection (Fig. 6A). Tumor uptake was decreased in the group treated with the blocking agent ([^{64}Cu]NODAGA-BBN (block): 0.09±0.03% ID/g and [^{64}Cu]NODAGA-galacto-BBN (block): 0.14±0.05% ID/g) compared with the group that did not receive the blocking agent ([^{64}Cu]NODAGA-BBN: 1.23±0.70% ID/g and [^{64}Cu]NODAGA-galacto-BBN: 1.46±1.20% ID/g) (Fig. 6B).

Discussion

Here, for the first time, we evaluated BBN analogues radiolabeled with ^{64}Cu that contained a galactose moiety as a linker between the BBN peptide and NODAGA chelator. These analogues were designed to provide relatively low liver and high prostate tumor uptake. In order to investigate the effects of galactose moiety in BBN in systemic circulation, blood radioactivity concentration-time profiles of [^{64}Cu]NODAGA-BBN or [^{64}Cu]NODAGA-galacto-BBN were determined. The blood radioactivity level of [^{64}Cu]NODAGA-BBN was ~6 times higher than that of [^{64}Cu]NODAGA-galacto-BBN at steady state as shown in Fig. 2 and Table II. This result suggests that [^{64}Cu]NODAGA-galacto-BBN is faster excreted from blood circulation compared to that of [^{64}Cu]NODAGA-BBN. In the PET imaging and biodistribution analysis, [^{64}Cu]NODAGA-galacto-BBN was more favorable *in vivo* tumor retention and pharmacokinetic properties than [^{64}Cu]NODAGA-BBN (Figs. 4 and 5). In the biodistribution studies, the tumor uptake for [^{64}Cu]NODAGA-galacto-BBN was higher than the tumor uptake for [^{64}Cu]NODAGA-BBN at 1 and 3 h (3.26±0.53 vs. 1.62±0.23% at 1 h and 1.96±1.16 vs. 1.18±0.18% at 3 h, respectively). Moreover, the liver uptake for [^{64}Cu]NODAGA-galacto-BBN was lower than the liver uptake for [^{64}Cu]NODAGA-BBN from 1 to 72 h according to PET imaging (Fig. 5). In the biodistribution studies, liver uptake of [^{64}Cu]NODAGA-galacto-BBN was significantly lower than that of [^{64}Cu]NODAGA-BBN at 1 and 3 h (1.13±0.19 vs. 2.69±0.69 at 1 h and 0.82±0.35 vs. 2.47±0.23% at 3 h, respectively) (Fig. 4). The tumor/blood ratios for [^{64}Cu]NODAGA-galacto-BBN are higher at 1 h (19.05±10.82) and 3 h (24.89±10.36) to any previously reported results in [^{64}Cu]NO2A-(AMBA)-BBN (2.6 at 24 h) (22), [^{64}Cu]NOTA-Bn-SCN-Aoc-BBN (18.029 at 4 h) (31), and [^{64}Cu]DOTA-amino acid linker-BBN (~4-8) (23). The favorable tumor/blood ratio of [^{64}Cu]NODAGA-galacto-BBN might be due to its fast clearance from systemic circulation as shown in Fig. 2. These pharmacokinetic properties might be caused by use of NODAGA and galactose as a chelator and a linker, respectively. i) NODAGA as a chelator; The group of Rogers hypothesized that a six-coordinate ^{64}Cu-labeled NOTA-Bn-SCN-Aoc-BBN would have greater *in vivo* stability than five-coordinate ^{64}Cu-labeled NO2A-Aoc-BBN and tumor/blood ratio of six-coordinate complex at 4 h after injection was found to be 18 (31). NODAGA is a chelator that can form with ^{64}Cu to six-coordinated state. However, the formation of six-coordinated structure of NODAGA with ^{64}Cu in [^{64}Cu]NODAGA-BBN or [^{64}Cu]NODAGA-galacto-BBN *in vivo* state must be determined in further study. ii) Galactose as a linker; the improved tumor/blood ratios of [^{64}Cu]NODAGA-galacto-BBN might be a role of galactose as a linker. Generally, purpose of linker insertion in radiometal-labeled peptide analogues could be the enhancement of *in vivo* stability or targeting efficiency. The use of galactose as a linker could reduce the lipophilicity of the conjugate, reduce liver accumulation and result in fast excretion of radioactivity.

Radiolabeling NODAGA-BBN with ^{64}Cu is simple. Previously, Liu *et al* developed a PET probe using NODAGA-RM1 and NODAGA-AMBA as a BBN analogue with ^{64}Cu; this strategy provided a radiochemical yield of >85% (32). In the current study, [^{64}Cu]NODAGA-BBN and [^{64}Cu]NODAGA-galacto-BBN were obtained with higher radiochemical yields (>99%) after incubation at 70˚C for 20 min (Table I). After labeling with ^{64}Cu, NODAGA-BBN and NODAGA-galacto-BBN were very stable in both human and mouse serum at 37˚C for 1 h, demonstrating no de-radiometallation.

Mansi *et al* produced a new conjugate, RM2, with the chelator DOTA coupled to D-Phe-Gln-Trp-Ala-Val-Gly-His-Sta-Leu-NH_2 via cationic spacer 4-amino-1-carboxymethyl-piperidine for labeling with and presented [^{111}In]RM2 and [^{68}Ga]RM2 as ideal candidates for single photon emission computed tomography (SPECT) and PET agents, respectively (33). [^{68}Ga]DOTA-BBN, BAY86-7548 has been investigated for safety, metabolism, pharmacokinetics, biodistribution and radiation dosimetry in five healthy men (34), and applied to prostate cancer patients for detecting intraprostatic prostate cancer (35).

Peptides used as targeting molecules have been labeled with ^{64}Cu using various suitable chelators such as DOTA,

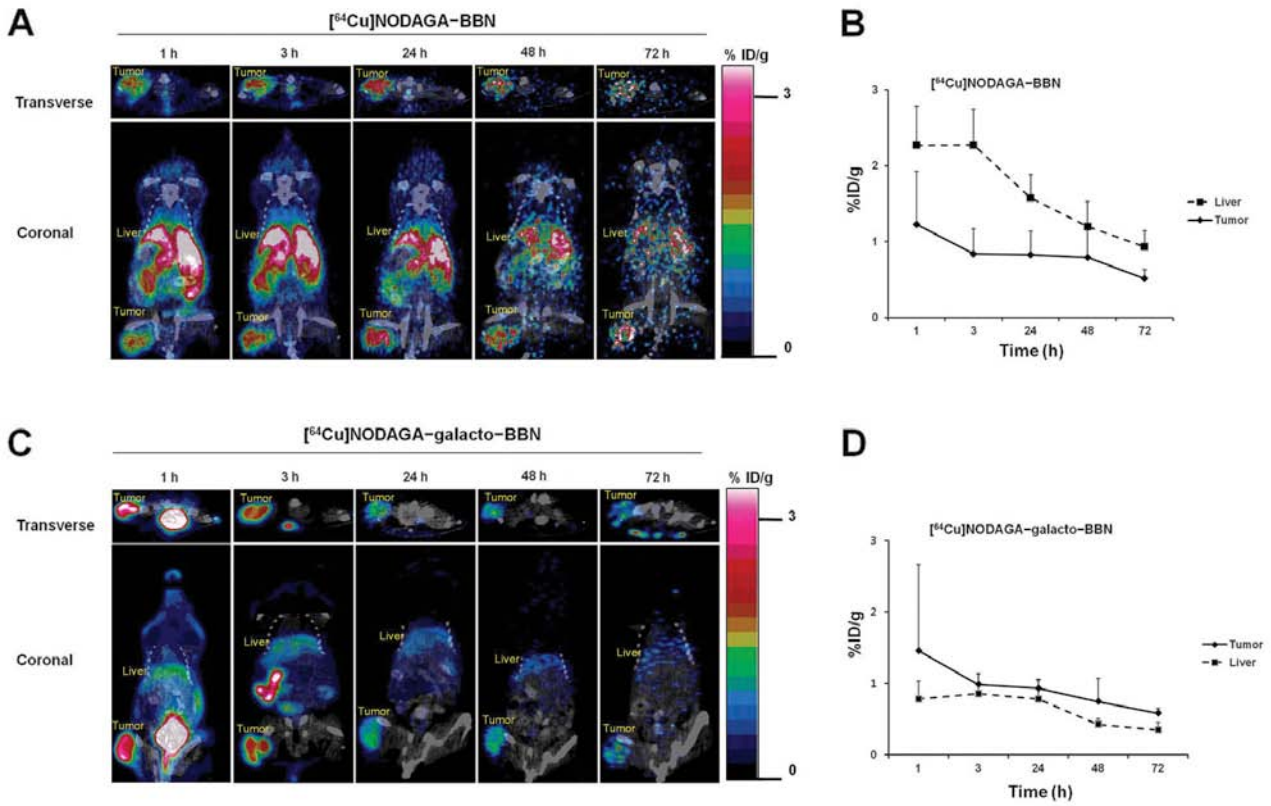

Figure 5. Small animal positron emission tomography (PET)/CT images of [^{64}Cu]1,4,7-triazacyclononane, 1-glutaric acid-4,7 acetic acid (NODAGA)-BBN and [^{64}Cu]NODAGA-galacto-BBN in PC3 human prostate cancer-bearing mice. (A and C) Decay-corrected whole-body transverse and coronal images were acquired at 1, 3, 24, 48 and 72 h after intravenous (i.v.) injection with 11.1-18.5 MBq of (A) [^{64}Cu]NODAGA-BBN (n=3) or (C) [^{64}Cu]NODAGA-galacto-BBN (n=3). L, liver; T, tumor. (B and D) Radioactivity curves for the tumor (closed diamond) and liver (closed square) were constructed using PET images after injection of 11.1-18.5 MBq of (B) [^{64}Cu]NODAGA-BBN and (D) [^{64}Cu]NODAGA-galacto-BBN from 1 to 72 h. Radioactivity was determined by region of interest (ROI) analysis and presented as percent of injected dose per gram (% ID/g) [mean ± standard deviation (SD)].

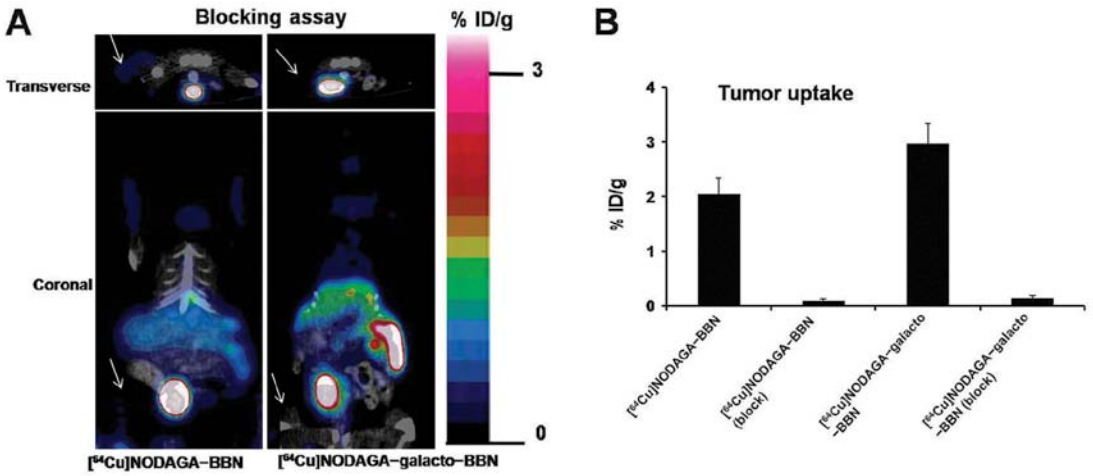

Figure 6. Small animal positron emission tomography (PET) imaging using a blocking agent. (A) Decay-corrected whole-body transverse and coronal small animal PET images at 1 h after injection with [^{64}Cu]1,4,7-triazacyclononane, 1-glutaric acid-4,7 acetic acid (NODAGA)-BBN, [^{64}Cu]NODAGA-galacto-BBN and NODAGA-BBN (15 mg/kg) or NODAGA-galacto-BBN (15 mg/kg) as the blocking agent. Arrows indicate the tumor site. (B) Comparison between uptake of [^{64}Cu]NODAGA-BBN and that of [^{64}Cu]NODAGA-galacto-BBN in PC3 tumors with or without NODAGA-BBN- or NODAGA-galacto-BBN-blocking agents. Radioactivity was determined by region of interest (ROI) analysis and presented as % ID/g [mean ± standard deviation (SD)].

NOTA, and NO2A including NODAGA (13,14,32,36). Improved *in vivo* kinetics is important for ^{64}Cu-based PET imaging and therapy. Clearly, the targeting efficiency of [^{64}Cu] NODAGA-galacto-BBN to PC3 tumor might be not superior to previously reported data (22,23,32). However, this study demonstrates that use of galactose and NODAGA in complex could induce the favorable pharmacokinetic characteristic such as rapid clearance from systemic circulation. Given its serum stability *in vitro* and favorable *in vivo* tumor-targeting properties (Figs. 3 and 4), [^{64}Cu]NODAGA-galacto-BBN warrants

further investigation for clinical translation. Additionally, ^{67}Cu ($t_{1/2}$=61 h) has favorable therapeutic β energy (100%, E_{β^-max}=577 keV, E_γ=195 keV), and nearly equivalent to ^{64}Cu in coordination chemistry. Moreover, the *in vivo* kinetics of ^{67}Cu-labeled molecules can be predicted with ^{64}Cu-labeled compounds (37). Thus, ^{67}Cu-labeled BBN analogues may be utilized for radiotherapy of GRPR-expressing tumors. In conclusion, NODAGA-BBN and NODAGA-galacto-BBN have been successfully prepared and radiolabeled with ^{64}Cu. The radiolabeling procedures were simple and straightforward. Both [^{64}Cu]NODAGA-BBN and [^{64}Cu]NODAGA-galacto-BBN stable against *in vitro* de-radiometallation and showed excellent *in vivo* tumor-targeting properties. In further studies, we will perform precise evaluation and characterization of these PET probes *in vitro* and *in vivo*.

Acknowledgements

This study was supported by the Nuclear R&D (grant code: NRF-2012M2A2A7013480 and NRF-2012M2A2A7013722) Programs of NRF, funded by MEST.

References

1. Ferlay J, Shin HR, Bray F, Forman D, Mathers C and Parkin DM: Estimates of worldwide burden of cancer in 2008: GLOBOCAN 2008. Int J Cancer 127: 2893-2917, 2010.
2. Feldman BJ and Feldman D: The development of androgen-independent prostate cancer. Nat Rev Cancer 1: 34-45, 2001.
3. Stangelberger A, Schally AV and Djavan B: New treatment approaches for prostate cancer based on peptide analogues. Eur Urol 53: 890-900, 2008.
4. Fischer R, Hill RM and Warshay D: Effects of psychodysleptic drug psilocybin on visual perception. Changes in brightness preference. Experientia 25: 166-169, 1969.
5. Nagalla SR, Barry BJ, Falick AM, Gibson BW, Taylor JE, Dong JZ and Spindel ER: There are three distinct forms of bombesin. Identification of [Leu13]bombesin, [Phe13]bombesin, and [Ser3,Arg10,Phe13]bombesin in the frog Bombina orientalis. J Biol Chem 271: 7731-7737, 1996.
6. Albrecht M, Doroszewicz J, Gillen S, Gomes I, Wilhelm B, Stief T and Aumüller G: Proliferation of prostate cancer cells and activity of neutral endopeptidase is regulated by bombesin and IL-1beta with IL-1beta acting as a modulator of cellular differentiation. Prostate 58: 82-94, 2004.
7. Aprikian AG, Tremblay L, Han K and Chevalier S: Bombesin stimulates the motility of human prostate-carcinoma cells through tyrosine phosphorylation of focal adhesion kinase and of integrin-associated proteins. Int J Cancer 72: 498-504, 1997.
8. Nagakawa O, Ogasawara M, Fujii H, Murakami K, Murata J, Fuse H and Saiki I: Effect of prostatic neuropeptides on invasion and migration of PC-3 prostate cancer cells. Cancer Lett 133: 27-33, 1998.
9. Bologna M, Festuccia C, Muzi P, Biordi L and Ciomei M: Bombesin stimulates growth of human prostatic cancer cells in vitro. Cancer 63: 1714-1720, 1989.
10. Ishimaru H, Kageyama Y, Hayashi T, Nemoto T, Eishi Y and Kihara K: Expression of matrix metalloproteinase-9 and bombesin/gastrin-releasing peptide in human prostate cancers and their lymph node metastases. Acta Oncol 41: 289-296, 2002.
11. Festuccia C, Angelucci A, Gravina G, Eleuterio E, Vicentini C and Bologna M: Bombesin-dependent pro-MMP-9 activation in prostatic cancer cells requires beta1 integrin engagement. Exp Cell Res 280: 1-11, 2002.
12. Markwalder R and Reubi JC: Gastrin-releasing peptide receptors in the human prostate: relation to neoplastic transformation. Cancer Res 59: 1152-1159, 1999.
13. Fournier P, Dumulon-Perreault V, Ait-Mohand S, Langlois R, Bénard F, Lecomte R and Guérin B: Comparative study of ^{64}Cu/NOTA-[D-Tyr6,βAla11,Thi13,Nle14]BBN(6-14) monomer and dimers for prostate cancer PET imaging. EJNMMI Res 2: 8, 2012.
14. Zhang H, Abiraj K, Thorek DL, Waser B, Smith-Jones PM, Honer M, Reubi JC and Maecke HR: Evolution of bombesin conjugates for targeted PET imaging of tumors. PLoS One 7: e44046, 2012.
15. Varasteh Z, Aberg O, Velikyan I, Lindeberg G, Sörensen J, Larhed M, Antoni G, Sandström M, Tolmachev V and Orlova A: In vitro and in vivo evaluation of a ^{18}F-labeled high affinity NOTA conjugated bombesin antagonist as a PET ligand for GRPR-targeted tumor imaging. PLoS One 8: e81932, 2013.
16. Baidoo KE, Lin KS, Zhan Y, Finley P, Scheffel U and Wagner HN Jr: Design, synthesis, and initial evaluation of high-affinity technetium bombesin analogues. Bioconjug Chem 9: 218-225, 1998.
17. Karra SR, Schibli R, Gali H, Katti KV, Hoffman TJ, Higginbotham C, Sieckman GL and Volkert WA: ^{99m}Tc-labeling and in vivo studies of a bombesin analogue with a novel water-soluble dithiadiphosphine-based bifunctional chelating agent. Bioconjug Chem 10: 254-260, 1999.
18. La Bella R, Garcia-Garayoa E, Langer M, Bläuenstein P, Beck-Sickinger AG and Schubiger PA: In vitro and in vivo evaluation of a ^{99m}Tc(I)-labeled bombesin analogue for imaging of gastrin releasing peptide receptor-positive tumors. Nucl Med Biol 29: 553-560, 2002.
19. La Bella R, Garcia-Garayoa E, Bahler M, Bläuenstein P, Schibli R, Conrath P, Tourwé D and Schubiger PA: A ^{99m}Tc(I)-postlabeled high affinity bombesin analogue as a potential tumor imaging agent. Bioconjug Chem 13: 599-604, 2002.
20. Rogers BE, Bigott HM, McCarthy DW, Della Manna D, Kim J, Sharp TL and Welch MJ: MicroPET imaging of a gastrin-releasing peptide receptor-positive tumor in a mouse model of human prostate cancer using a ^{64}Cu-labeled bombesin analogue. Bioconjug Chem 14: 756-763, 2003.
21. Parry JJ, Andrews R and Rogers BE: MicroPET imaging of breast cancer using radiolabeled bombesin analogs targeting the gastrin-releasing peptide receptor. Breast Cancer Res Treat 101: 175-183, 2007.
22. Lane SR, Nanda P, Rold TL, Sieckman GL, Figueroa SD, Hoffman TJ, Jurisson SS and Smith CJ: Optimization, biological evaluation and microPET imaging of copper-64-labeled bombesin agonists, [^{64}Cu-NO2A-(X)-BBN(7-14)NH2], in a prostate tumor xenografted mouse model. Nucl Med Biol 37: 751-761, 2010.
23. Parry JJ, Kelly TS, Andrews R and Rogers BE: In vitro and in vivo evaluation of ^{64}Cu-labeled DOTA-linker-bombesin(7-14) analogues containing different amino acid linker moieties. Bioconjug Chem 18: 1110-1117, 2007.
24. Haubner R, Wester HJ, Weber WA, Mang C, Ziegler SI, Goodman SL, Senekowitsch-Schmidtke R, Kessler H and Schwaiger M: Noninvasive imaging of alpha(v)beta3 integrin expression using ^{18}F-labeled RGD-containing glycopeptide and positron emission tomography. Cancer Res 61: 1781-1785, 2001.
25. Haubner R, Wester HJ, Burkhart F, Senekowitsch-Schmidtke R, Weber W, Goodman SL, Kessler H and Schwaiger M: Glycosylated RGD-containing peptides: tracer for tumor targeting and angiogenesis imaging with improved biokinetics. J Nucl Med 42: 326-336, 2001.
26. Haubner R, Kuhnast B, Mang C, Weber WA, Kessler H, Wester HJ and Schwaiger M: [^{18}F]Galacto-RGD: synthesis, radiolabeling, metabolic stability, and radiation dose estimates. Bioconjug Chem 15: 61-69, 2004.
27. Haubner R, Weber WA, Beer AJ, Vabuliene E, Reim D, Sarbia M, Becker KF, Goebel M, Hein R, Wester HJ, Kessler H and Schwaiger M: Noninvasive visualization of the activated alphavbeta3 integrin in cancer patients by positron emission tomography and [^{18}F]Galacto-RGD. PLoS Med 2: e70, 2005.
28. Wu AM, Yazaki PJ, Tsai Sw, Nguyen K, Anderson AL, McCarthy DW, Welch MJ, Shively JE, Williams LE, Raubitschek AA, Wong JY, Toyokuni T, Phelps ME and Gambhir SS: High-resolution microPET imaging of carcinoembryonic antigen-positive xenografts by using a copper-64-labeled engineered antibody fragment. Proc Natl Acad Sci USA 97: 8495-8500, 2000.
29. Williams HA, Robinson S, Julyan P, Zweit J and Hastings D: A comparison of PET imaging characteristics of various copper radioisotopes. Eur J Nucl Med Mol Imaging 32: 473-480, 2005.
30. Kim JY, Park H, Lee JC, Kim KM, Lee KC, Ha HJ, Choi TH, An GI and Cheon GJ: A simple Cu-64 production and its application of Cu-64 ATSM. Appl Radiat Isot 67: 1190-1194, 2009.

31. Craft JM, De Silva RA, Lears KA, Andrews R, Liang K, Achilefu S and Rogers BE: In vitro and in vivo evaluation of a ^{64}Cu-labeled NOTA-Bn-SCN-Aoc-bombesin analogue in gastrin-releasing peptide receptor expressing prostate cancer. Nucl Med Biol 39: 609-616, 2012.
32. Liu Y, Hu X, Liu H, Bu L, Ma X, Cheng K, Li J, Tian M, Zhang H and Cheng Z: A comparative study of radiolabeled bombesin analogs for the PET imaging of prostate cancer. J Nucl Med 54: 2132-2138, 2013.
33. Mansi R, Wang X, Forrer F, Waser B, Cescato R, Graham K, Borkowski S, Reubi JC and Maecke HR: Development of a potent DOTA-conjugated bombesin antagonist for targeting GRPr-positive tumours. Eur J Nucl Med Mol Imaging 38: 97-107, 2011.
34. Roivainen A, Kähkönen E, Luoto P, Borkowski S, Hofmann B, Jambor I, Lehtiö K, Rantala T, Rottmann A, Sipilä H, Sparks R, Suilamo S, Tolvanen T, Valencia R and Minn H: Plasma pharmacokinetics, whole-body distribution, metabolism, and radiation dosimetry of ^{68}Ga bombesin antagonist BAY 86-7548 in healthy men. J Nucl Med 54: 867-872, 2013.
35. Kähkönen E, Jambor I, Kemppainen J, Lehtiö K, Grönroos TJ, Kuisma A, Luoto P, Sipilä HJ, Tolvanen T, Alanen K, Silén J, Kallajoki M, Roivainen A, Schäfer N, Schibli R, Dragic M, Johayem A, Valencia R, Borkowski S and Minn H: In vivo imaging of prostate cancer using [^{68}Ga]-labeled bombesin analog BAY86-7548. Clin Cancer Res 19: 5434-5443, 2013.
36. Jackson AB, Nanda PK, Rold TL, Sieckman GL, Szczodroski AF, Hoffman TJ, Chen X and Smith CJ: ^{64}Cu-NO2A-RGD-Glu-6-Ahx-BBN(7-14)NH2: a heterodimeric targeting vector for positron emission tomography imaging of prostate cancer. Nucl Med Biol 39: 377-387, 2012.
37. Park JA and Kim JY: Recent advances in radiopharmaceutical application of matched-pair radiometals. Curr Top Med Chem 13: 458-469, 2013.